SIMULATION OF DDT IN HYDROGEN-AIR BEHIND A SINGLE OBSTACLE

Gaathaug A.V.[1], Vaagsaether K.[1] and Bjerketvedt, D.[1]
[1] Telemark University College, Faculty of Technology, P.O.Box 203, Porsgrunn, 3901, Norway, andre.v.gaathaug@ hit.no

ABSTRACT

Two-dimensional numerical simulations of detonation deflagration transition (DDT) in hydrogen-air mixtures are presented and compared with experiments. The investigated geometry was a 3 meter long square channel. One end was closed and had a single obstacle placed 1 m from the end, and the other end was open to the atmosphere. The mixture was ignited at the closed end. Experiments and simulations showed that DDT occurred within 1 meter behind the obstacle. The onset of detonation followed a series of local explosions occurring far behind the leading edge of the flame in a layer of unburned reactants between the flame and the walls. A local explosion was also seen in the experiments, and the pressure records indicated that there may have been more. Furthermore, local explosions were observed in the experiments and simulations which did not detonate. The explosions should have sufficient strength and should explode in a layer of sufficient height to result in a detonation.

The numerical resolution was 0.5 mm per square cell, and further details of the combustion model used are provided in the paper.

1.0 BACKGROUND

This paper describes a numerical study of detonation deflagration transition (DDT) in a turbulent jet behind an obstacle. Numerical and experimental results were compared for similar cases. Fig. 1 shows the dimensions for the geometry used in this investigation. The 3 meter long channel had a 0.1 x 0.1 m^2 square cross section with transparent sidewalls and smooth top and bottom walls made of painted steel. One end was closed and one end was open to the atmosphere. The channel was filled with a mixture of hydrogen and air. The gas mixture was ignited at the closed end, and the combustion propagated one meter before reaching an obstacle. A jet formed at the obstacle opening and DDT was observed behind the obstacle. Prior to DDT some local explosions occurred in a layer between the flame and the walls.

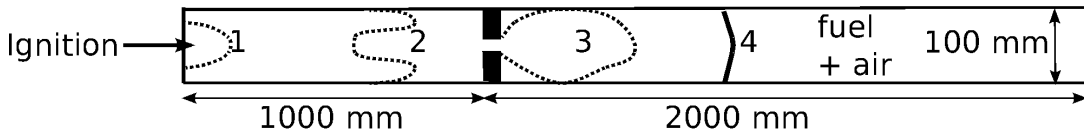

Figure 1. Investigated geometry. 1-3 represent the deflagration, while 4 represents the detonation. In some experiments DDT was observed behind the obstacle.

The earliest observations of detonations were conducted by Mallard and Le Chatelier in 1881 [1] and by Berthelot and Vielle [2] about the same time. Chapman [3] and Jouguet [4] formulated the so-called CJ theory of detonations, a one-dimensional theory combining the conservation of mass, momentum, and energy with an equation of state and an assumption of an infinitely fast reaction. The CJ theory results in two limiting solutions, one for detonations and one for deflagrations.

An expansion of the CJ theory for detonations was developed almost simultaneously by Zeldovich, von Neumann, and Döring [5]. Known as the one-dimensional ZND theory, it accounts for the chemical reaction time and length of a shock wave that propagates in front of the reaction. The shock

wave occurs first followed by an induction zone. Behind the induction zone there is an exothermic reaction zone where the chemical energy is converted to heat. As the chemical reactions reach equilibrium its state could be the same as the CJ state.

Urtiew and Oppenheim [6] conducted a series of classical experiments in smooth channels in which they observed DDT as the flame accelerated in the channel. DDT was observed at the leading edge of the flame front behind a precursor shock, and also at the shock wave itself as the flame caught up with the front. They also observed DDT at the contact surface as two shock waves merged. Lee [7] noted that the flame should reach a velocity close to the speed of sound in the products prior to DDT.

Knystautas et al. [8] investigated DDT in a turbulent jet, as a flame propagated from a small chamber through a circular or rectangular opening into a large detonation chamber. They varied the size and shape of the opening and concluded that three criteria were necessary for DDT to occur. First is the presence of sufficiently large scale energetic turbulent eddies, and second is sufficient small scale turbulence to promote mixing. The third criterion is that gradients of induction time must be generated inside a turbulent eddy, permitting DDT to occur in the eddy. The size of the eddy should be on the order of the cell size of the detonation. Thomas and Jones [9] later argued that the time scale is too short for conduction to occur between products and fresh reactants, and that the high shear stress in the flame front caused mixing at the length scale of the flame thickness. This resulted in increased energy release in the flame front, which in turn led to auto-ignition of the unburned gas and the development of a hot spot transition. Large scale jet initiation experiments were performed by Moen et al. [10]. Their experimental setup consisted of a steel tube with one end closed and a plastic bag attached to the open end. The tube and bag were filled with acetylene and air and ignited at the closed end. They examined the cases where the open end of the tube was completely open, centrally blocked, or opened with an orifice plate. They observed DDT as deflagration propagated through the opening into the plastic bag. In some experiments DDT was observed at the ground or near the plastic boundary.

DDT has been observed in channels and pipes with internal obstacles, often referred to as obstructed channels. Early work showed that the detonations in these channels and pipes could propagate with velocities less than half the CJ velocity. These were called quasi-detonations, and Teodorczyk et al. [11] described their propagation mechanism. As the detonation passes through one obstacle, it diffracts and dies. Then the shock wave propagates and reflects off the next obstacle and initiates a new detonation. This continues along the channel. Teodorczyk et al. studied hydrogen and oxygen mixtures and acetylene and propane mixtures.

Knystautas et al. [12] studied flame acceleration in an obstructed pipe followed by a section of smooth pipe. They observed that the flame needed to accelerate to about half the CJ velocity before DDT occurred in the smooth section. In some of their experiments they observed that the flame accelerated initially, but then failed to accelerate further and develop into a detonation.

Many researchers have investigated the onset of detonation and the transition from deflagration to detonation. Zeldovich et al. [13] and Lee et al. [14] stated the need for a gradient of induction time, and that the reaction must propagate in this gradient. The gradient must be coherent with a shock wave in front of it. Further, the reaction must not be too fast or too slow compared to the shock wave, otherwise it can fail. A thorough review of DDT and flame acceleration was conducted by Ciccarelli and Dorofeev [15].

Numerical simulations of dispersion, explosions, and the details of detonation and DDT have been performed by many researchers since computers became available in the 1960s. A main principle of these simulations is the solution of mass, momentum, and energy conservation. Turbulence and chemical reactions have also been included using different methods. Simulations of hydrogen safety problems were performed by Brennan et al. [16] and Middha [17], among others. Brennan investigated hydrogen jets using Large Eddy Simulation (LES), and showed that the flame length varied with initial nozzle turbulence. Middha used the FLACS code to simulate several cases related to hydrogen safety; he also developed models to indicate the possibility of DDT. Gamezo et al. [18] simulated DDT and

detonations in an obstructed channel similar to Teodorczyk's experiments [11]. They showed that the detonation originated in hot spots behind the reflected shock waves and that the distance from ignition to DDT scaled linearly with the squared channel height.

The present work continues earlier work by Vaagsaether et al. [19] and Knudsen et al. [20]. Their goal was to determine where DDT occurred in a configuration with a single obstacle. The present work differs from smooth tube DDT experiments in that it has one obstacle which generates a confined jet. It also differs from the earlier studies on unconfined jets, since in the present case the jet is confined allowing DDT to be related to the explosions between the flame and the walls. Also, the present work does not include the reflections of shock waves from repeated obstacles as are seen in obstructed channel experiments.

2.0 NUMERICAL METHOD

The numerical investigations were conducted with Vaagsaether's FLIC code, which is a 2D flux limited centred TVD method. A detailed background on the method is provided by Toro [21] and Vaagsaether [19]. FLIC solves the Euler equations with the ideal gas equation of state. The turbulence is solved by conserving the turbulent kinetic energy *k*, with sources and sinks [19]. The combustion model is a progress variable method where β is conserved and can represent a normalized concentration, see (1). β varies between 1 and 0, where 1 is burnt gas and 0 is fresh gas.

$$\frac{\partial \rho \beta}{\partial t} + \nabla(\rho u \beta) = \dot{\varpi} \qquad \textbf{(1)}$$

$$\frac{\partial \rho \alpha}{\partial t} + \nabla(\rho u \alpha) = \dot{\vartheta} \qquad \textbf{(2)}$$

Another progress variable, α, varies from 0 to 1 and represents the induction time, see (2). The induction time variable is not connected to the conservation of energy, as it is assumed that the induction reaction's heat of reaction is zero.

The reaction rate $\dot{\varpi}$ is a combination of a turbulence controlled rate and a chemical kinetic rate, see (3).

$$\dot{\varpi} = \max[\dot{\varpi}_T, \dot{\varpi}_k]$$
$$\dot{\varpi}_T = \rho_u S_T \sqrt{\left(\frac{\partial \beta}{\partial x}^2 + \frac{\partial \beta}{\partial y}^2\right)} \qquad \textbf{(3)}$$

The turbulent burning velocity S_T uses Flohr and Pitsch's model [22]. This model (4) includes a constant *A* set to 0.52 [22].

$$S_T = S_L\left(1 + A\frac{\sqrt{\mathrm{Re}\cdot \mathrm{Pr}}}{Da^{0.25}}\right) \qquad \textbf{(4)}$$

Re, *Pr*, and *Da* are the subgrid Reynolds, Prandtl, and Damköhler numbers, respectively. The Iijima and Takeno [23] model for the laminar burning velocity S_L is used. The chemical kinetic rate $\dot{\varpi}_k$ is a two step model [24] in which the first step has zero heat of reaction and the second step is exothermic. The total chemical kinetics is obtained from (6) and (7).

$$\dot{\vartheta} = f(p,T) = \frac{\rho}{\tau} \tag{5}$$

$$\dot{\omega}_k = \begin{Bmatrix} 0 & if\ \alpha < 1 \\ \rho\left(A_\beta p^2 \beta^2 \exp\left[\frac{-T_{a,\beta}}{T} \right] - A_\beta p^2 (1-\beta)^2 \exp\left[-\left(\frac{T_{a,\beta}}{T} + \frac{q}{RT} \right) \right] \right) & if\ \alpha = 1 \end{Bmatrix} \tag{6}$$

The present work uses two induction time models for $\dot{\vartheta}$, (5) and (7). One model was presented by Sichel et al. [25] and the other by del Alamo and Williams [26].

$$\begin{aligned} \tau_{Sich} &= A_\alpha \frac{T}{p} \exp\left[-B_\alpha + \frac{C_\alpha}{T} + D_\alpha \left(\frac{p}{p_{atm}} \right)^2 \exp\left(\frac{T_{a,\alpha}}{T} \right) \right] \\ \tau_{delAlamo} &= \frac{1}{c_{O_2}\left(2k_1 - k_{10}c_M\right)} \ln\left[\left(2k_1 - k_{10}c_M\right) \cdot \frac{c_{H_2} k_2 k_3}{2 c_{O_2} k_1 k_{12b}} \right] \end{aligned} \tag{7}$$

Table 1. Model constants.

A_β	$1.05*10^{-5}$ [s^{-1} Pa^{-2}]
$T_{a,\beta}$	2000 [K]
A_α	$6.2335*10^{10}$ [Pa K^{-1} s]
B_α	35.1715 [-]
C_α	8530.6 [K]
D_α	$7.22*10^{-11}$ [-]
$T_{a,\alpha}$	21205 [K]

The model constants for the del Alamo model are given in [38].

Two step kinetics is selected for the modelling of DDT and detonations. If the unburned mixture is sufficiently heated or compressed and α = 1, then an exothermic reaction will begin. It is important to model the induction time for detonations, since the detonation wave consists of shock compression and a subsequent reaction zone. Detonations and DDT have also been studied successfully with one step chemical kinetics in cases where the spatial resolution is high. The spatial resolution of the present work is assumed to be too coarse for one step kinetics [29].

3.0 EXPERIMENTAL AND NUMERICAL SETUP

A sketch of the experimental setup is provided in Figure 1, and the basic configuration is described in the Background section. The channel's single obstacle was placed 1 m from the closed end. The obstacle opening was a rectangular slit extending across the entire width of the channel that was adjustable to enable changes in the blockage ratio (BR=blocked area/total area). In the experiment, hydrogen-air mixtures filled the channel by adjusting the flow rates of air and hydrogen and flushing the mixture through the channel from the inlet at the closed end. The mixtures had a hydrogen concentration between 15% and 35%. All experiments were performed at ambient pressure and temperature. A 10 kV spark was used to ignite the mixtures at the closed end. The pressures were recorded by two Kistler 7001 pressure transducers placed in the section in front of the obstacle. Three Kistler 603b transducers were mounted at 200 mm, 600 mm, and 1000 mm behind the obstacle. The flame propagation was recorded by a Photron SA1 high speed camera recording at 30000 fps.

The geometry of the numerical setup was similar to that of the experimental setup. The domain was 2D and 3 m in length, with solid reflecting top and bottom boundaries. The outlet was a zero gradient

boundary. The internal geometry (i.e., the obstacle) was solid and reflecting. The initial conditions and parameters are listed in Table 2. The subscripts u and b refer to unburned and burned.

Table 2. Parameters for the numerical simulation.

Parameter	**30% H_2**	**35% H_2**
$M_{w,u}$ Unburned Molecular weight [kg/mol]	$20.9*10^{-3}$	$19.5*10^{-3}$
$M_{w,b}$ Burned Molecular weight [kg/mol]	$24.1*10^{-3}$	$22.4*10^{-3}$
ρ_0 Initial density [kg/m^3]	0.85	0.8
γ_u Unburned adiabatic index [-]	1.4	1.4
γ_b Burned adiabatic index [-]	1.242	1.243
q Change of enthalpy of reactants [J/kg]	$3.01*10^6$	$3.21*10^6$
p_0 Initial pressure [Pa]	$1*10^5$	
$u_x = u_y$ Initial velocity [m/s]	0	
α_0 Initial induction progress variable [-]	0	
β_0 Initial reaction progress variable (except ignition) [-]	0	
dx Size of computational cell [mm]	0.5	

A relatively coarse mesh of 0.5 mm in 2D was chosen due to computational time and resource constraints.

4.0 EXPERIMENTAL RESULTS

A description of the flame propagation up to the obstacle was presented in a prior publication [27]. To summarize, after ignition the flame propagated towards the obstacle and then inverted several times. Relatively low flame speeds were observed (average 40 m/s), and the flame propagation was recorded using high speed schlieren images. The pressure records and flame position are shown in Figure 2. The blockage ratio was BR=0.9, and the section behind the obstacle was too short (0.5 m) to achieve DDT. In the present study a longer section is used behind the obstacle, and DDT has been observed for various BR values and gas mixture concentrations.

As the flame propagated towards the obstacle, it inverted and became a tulip flame. In the simulations, reproducing the flame shape before it reached the obstacle has proven to be a challenge.

The experimental study included variations in the blockage ratio and hydrogen concentrations. The lowest blockage (largest opening) was 0.5 (BR=5 cm blocked/10 cm total). The hydrogen concentrations varied from 15% (φ=0.4) to 35% (φ=1.3). The pressure histories were recorded, as were the positions along the length of the channel where DDT occurred.

As the flame propagated up to the obstacle, a jet was generated through the obstacle opening. As the flame reached the jet, its front accelerated relative to the lab frame. The flame speed was high in the length direction of the channel, but stagnated near the walls.

Using high speed film, local explosions and pressure waves could be interpreted as curved sections of bright light that move from one frame to the next. Some experiments showed DDT close to one wall along with its resulting self-propagating detonation wave. Fig. 3 shows a sequence of high speed frames. In the first two frames the flame propagated through the obstacle and into the channel behind it. In the third frame there appeared to be a local explosion developing at the top wall, while a pressure wave propagated downward and reflected off the bottom wall.

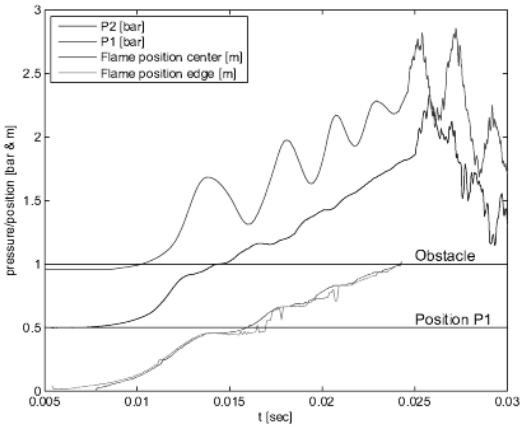

Figure 2. Pressure and flame position in the experiments, for the flame propagation before the obstacle. 30% H_2 in air and BR=0.9 [27].

The propagation of this pressure wave is seen in frames 4 and 5. Frame 6 shows a detonation (bright light) at the top of the channel. This bright light appeared about the same time as the pressure wave from the local explosion reached the flame front. In the last two frames the detonation grew to encompass the entire cross section of the channel.

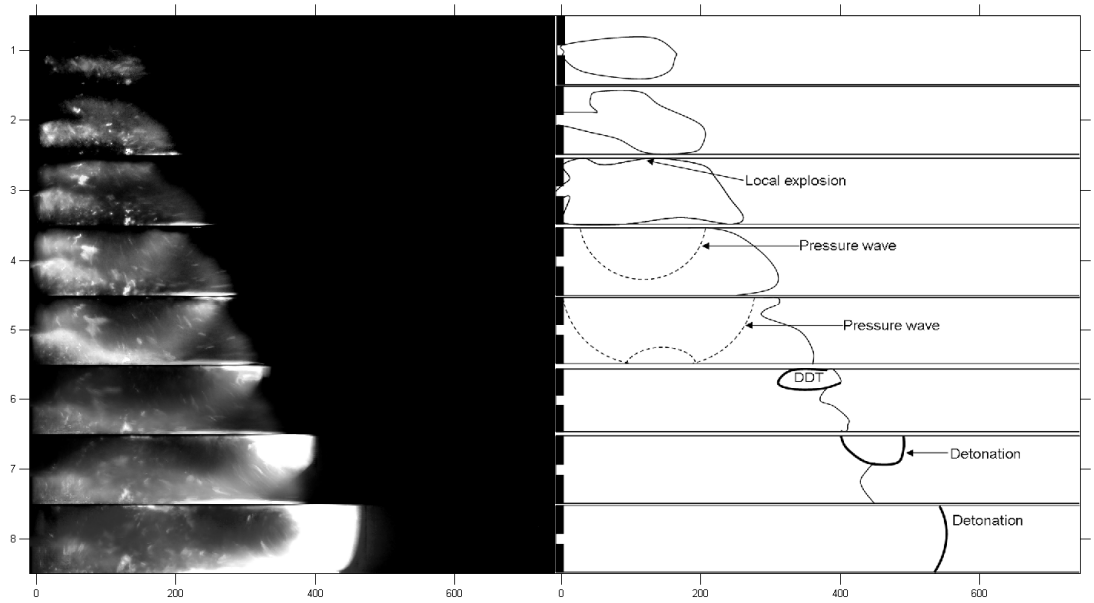

Figure 3. High speed frames with sketches of their phenomena. BR=0.84, H_2 conc. 35%, 30000 fps.

Fig. 4 shows the pressure records (recorded at the bottom wall) corresponding to Figure 3. The vertical lines correspond to the frames of Figure 3, and the pressure is offset a distance equal to the location of the transducer behind the obstacle (unit: dm).

Between frames 5 and 6 there was a significant pressure increase from the local explosion at the top wall. After frame 5 several pressure oscillations were recorded that were on the order of 0.5 bar. These were smaller than the detonation spikes (order of 30 bar) but still significantly larger than the measurement noise seen at the beginning of the pressure records. There was a pressure increase from frame 1 to 3, and a section of white light at the bottom wall was first visible in frame 2.

The experiments were repeatable as far as the trend of DDT occurrence vs. concentration and BR. However, the position of the onset varied even for equivalent concentrations and BRs. Some experiments did not result in DDT behind the obstacle. Fig. 5 shows frames from an experiment where DDT was not observed; the flame bubble seen at the front could have auto-ignited but failed to develop into a detonation. The pressure records from this experiment showed similar oscillations as in the case when DDT was observed.

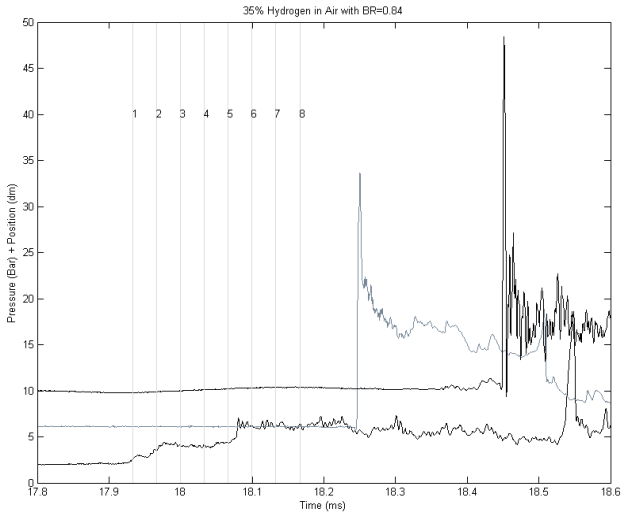

Figure 4. Pressure records for the experiment with BR=0.84 and H_2 conc. 35%. The pressure offset is equal to the distance of the transducer behind the obstacle. The vertical lines correspond to the frames in Figure 3.

5.0 NUMERICAL RESULTS

As stated earlier, the scope of this paper focuses on DDT in the flow and the reactions behind the obstacle. However, the numerical simulation included the entire channel geometry and time from ignition until all reactants were burned.

The numerical results were visualized using numerical schlieren-like frames (H). These were calculated from the density field at a single time instance, using (9) with k=25.

$$H = |\nabla \rho| \cdot \exp\left[-k \frac{|\nabla \rho|}{|\nabla \rho|_{\max}} \right] \qquad \textbf{(9)}$$

Results from one numerical simulation with BR=0.84 and H_2 conc. 35% are shown in Figure 6. As the flame propagated through the obstacle it became elongated. There was a thin layer between the flame and the wall in which several small explosions were seen. The first explosion was seen in frame 45, and it was followed by several small local explosions occurring in the volume between the walls and the flame. In frames 55 and 61 a fast reaction wave propagated in the bottom layer, and an oblique shock wave reflected at the top wall; this in turn started a fast reaction wave at the top wall (frame 67). The last two frames show a detonation.

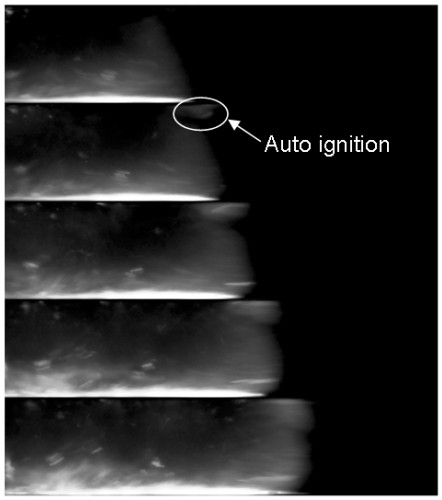

Figure 5. Experimental case with BR=0.84 and H_2 conc. 27%. A bubble was seen at the front of the flame but it did not develop into a detonation.

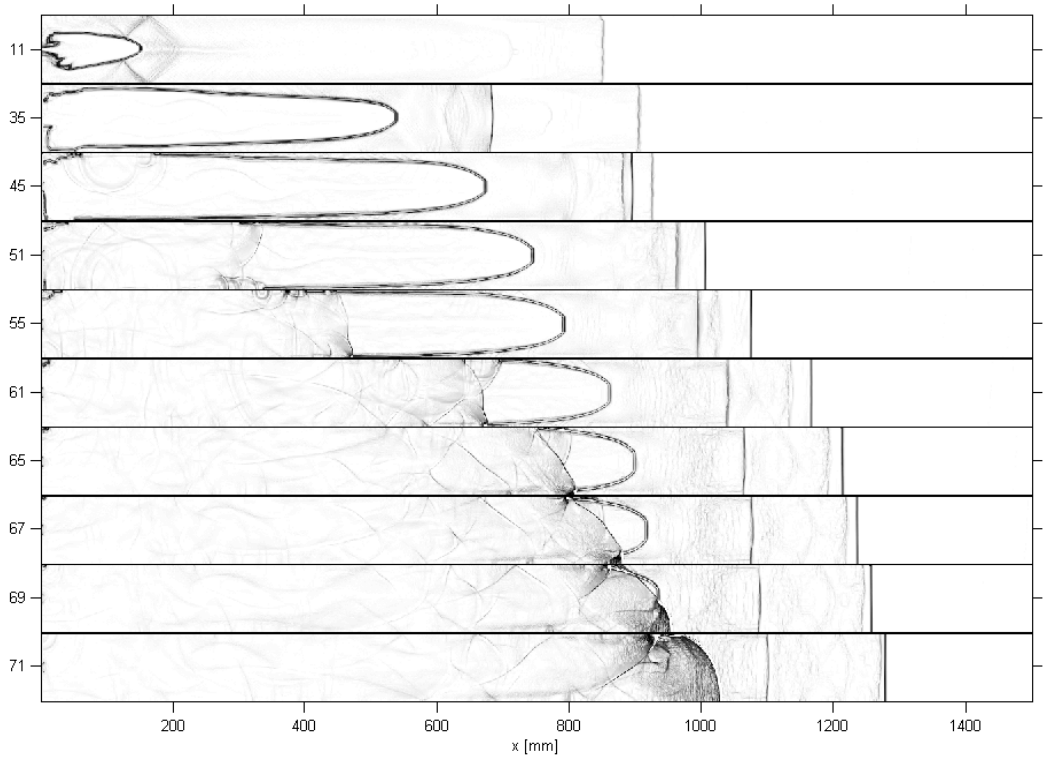

Figure 6. Numerical schlieren pictures from the simulation case with BR=0.84 and 35% H_2 in air. Frames are not equidistant in time. Induction model: del Alamo.

Figure 7 shows an x-t plot of $\partial p/\partial x$ along the bottom wall, where x is the length axis of the channel. The results can be seen as numerical streak-schlieren images at the bottom wall, for simulations where BR=0.75 and 35% H_2. Two cases with two different induction models are presented in Figure 7; one developed into a detonation while the other did not. The two cases used the same run up before the obstacle, but compared different induction models (del Alamo and Sichel) for the process behind the obstacle. There were many local explosions in both cases. The del Alamo model simulations exploded earlier than the Sichel model simulations. Also, for a given setup, the del Alamo simulations developed into a detonation while the Sichel model did not. The left image in Figure 7 shows three

local explosions that failed to develop into a detonation, at 300 mm, 500 mm, and 650 mm behind the obstacle. Similar behaviours were observed in other cases of detonation failure or success.

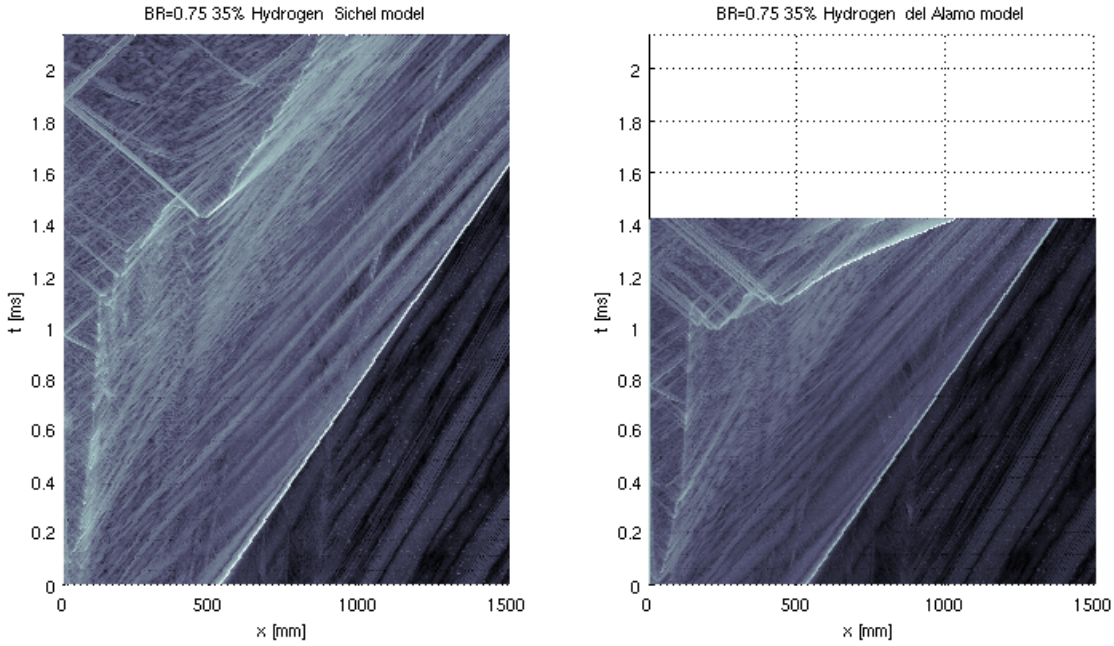

Figure 7. Numerical case with BR=0.75 and H_2 conc. 35%. Right image shows detonation with the del Alamo model; left image shows no detonation with the Sichel model. $(\partial p/\partial x)/(\partial p/\partial x)_{max}$ is shown in the figure.

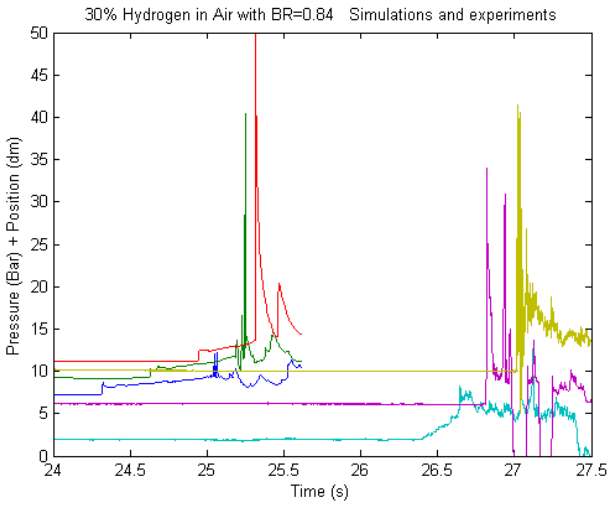

Figure 8. Comparison of pressure levels, with simulations on the left and experiments on the right. The pressure curves are offset equal to the position behind the obstacle (unit: dm).

Figure 8 compares the simulated and experimental pressure records. The simulated pressures (three on the left hand side) are lower for the first two transducers compared with the experimental measurements (right hand side). The pressure curves are offset on the pressure axis by a distance equal to that of the transducer behind the obstacle (in dm). The simulated pressures are recorded further behind the obstacle than the experimental pressures, since the simulated onset of detonation was further behind the obstacle than the experimental onset. The simulated pressure showed a shock propagating in front of the flame; this was also seen in the experiments at the first transducer.

In the simulated cases where DDT was not observed, there were still local explosions in the layer between the flame and the walls. This can be seen in frames 223, 281, and 323 in Figure 9; furthermore, there was a fast reaction wave in the layer as seen in frames 339, 391, and 407. However, this did not develop into a detonation.

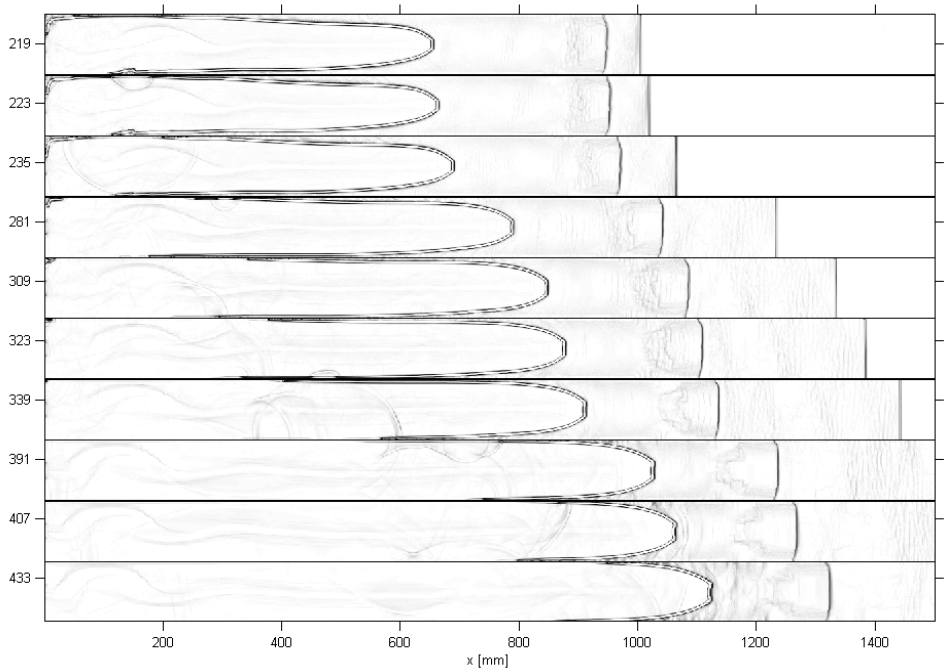

Figure 9. Simulated case with BR=0.75 and 30% H_2. No DDT in this case, but local explosions were still present.

5.0 DISCUSSION

Within the numerical simulations, local explosions can be described using the induction progress variable α that reaches α=1 in one cell, thus initiating the exothermic reaction. The relatively high temperatures in the layer between the wall and the flame are caused by the mixing of products and reactants, which leads to a reduced induction time. A high reaction rate follows and could result in a shock wave. Shock compression of the neighbouring cells could in turn result in the onset of detonation. Some of these explosions were observed in isolated islands of reactants or in too narrow layers of reactants with no detonation seen, but several explosions could add up and eventually lead to a detonation. Interactions between the top and bottom wall explosions were observed in simulations which lead to detonation. Local explosions were also seen in simulations which did not detonate, but they were too weak or occurred in layers which were too narrow or did not have the top/bottom wall interaction.

The experimental study showed some pressure waves recorded at the first transducer behind the obstacle prior to DDT. Usually there was one stronger wave and several smaller variations in pressure, which were still larger than the recorded noise. These could originate from small explosions similar to those seen in the simulations. The waves were also seen in experiments without DDT, but they could have been too weak to result in the onset of detonation.

A more detailed study of the phenomenon is required to draw further conclusions.

A bright layer along the bottom wall seen on the high speed film was common to all experiments with DDT and near the DDT limits (Figure 3 and Figure 5). One could speculate that this is similar to the fast reaction wave seen in the simulations. Future investigations of the pressure in this layer together

with schlieren photography are planned. The study of detonations in layers could be similar to the study by Dabora et al. [28] in which they studied detonations bounded by a wall and a compressible layer. They concluded that the velocity loss due to the expanding compressible layer could cause failure to propagate as a detonation. This loss was dependent on the density ratio of the gases used. As seen in the simulations, there is an oblique shock behind the fast reaction wave in the layer between the flame and the wall, which is similar to the case by Dabora et al.

The bubble seen in Figure 5 could be an auto-ignition from shock compression or the locally high reaction rate in the flame front. It fails to develop into a detonation, but this phenomenon was not seen directly in the simulations.

There is an obvious limitation to the 2D approximation used in the simulations, as the influence of corners is not considered in the simulations. The authors have earlier shown that the run up and flame propagation through the obstacle is three-dimensional. Buoyancy effects and non-uniform concentrations behind the obstacle were also not included.

The influence and validity of the induction models will also be investigated further in future work.

6.0 SUMMARY

- Simulations of DDT in hydrogen air mixtures were performed, using a cell size $\Delta x = 0.5$ mm
- The simulations were compared with pressure records and high speed video from experiments.
- DDT was observed in both experiments and simulations at the walls between 1200 mm and 2000 mm from the ignition end.
- Local explosions far behind the leading edge of the flame were observed in simulations and experiments. These explosions initiated the process of DDT. The simulations showed that the explosions occurred in a layer between the flame and the walls.
- Several explosions followed the first, and the fast reaction and the accelerating wave propagated along the walls and resulted in DDT in some simulations. In other simulations DDT was not observed; there were local explosions but the fast reaction wave died after several attempts. In some simulations the fast reaction wave accelerated in an isolated layer of reactants, where the wave died as it ran out of fresh gas.
- The local explosions must have sufficient strength and must propagate in a layer of sufficient height. The blast from an explosion at one wall can initiate a new explosion at the other wall.

REFERENCES

1. Mallard, E. and Le Chatelier, H., On the Propagation Velocity of Burning in Gaseous Explosive Mixtures, *C. R. Hebd. Seances Acad. Sci.*, No. 93, 1881, pp. 145-148.
2. Berthelot, M. and Vielle, P., On Explosive Waves, *C. R. Hebd. Seances Acad. Sci.*, No. 94, 1882, pp. 149-152.
3. Chapman, D.L., On the Rate of Explosion in Gases, *Philos. Mag.*, **47**, 1899, pp. 90-104.
4. Jouguet, E., On the Propagation of Chemical Reactions in Gases, *J. de Mathematiques Pures et Appliquees*, **1**, 1905, pp. 347-425.
5. Fickett, W. and Davis, W.C., Detonation: Theory and Experiments, 1979, University of California Press.
6. Urtiew, P. and Oppenheim, A.K., *Proc. R. Soc. Lond. A*, **295**, 1966.
7. Lee, J.H.S., The Detonation Phenomena, 2008, Cambridge University Press, New York.

8. Knystautas, R., Lee, J.H.S. and Moen, I., Direct Initiation of Spherical Detonation by a Hot Turbulent Gas Jet, 17th Symp. (Int.) on Combustion, Pittsburgh, PA, The Combustion Inst., 1979, pp. 1235-1245.
9. Thomas, G.O. and Jones, A., Some Observations of the Jet Initiation of Detonation, *Combustion and Flame*, **120**, 2000, pp. 392-398.
10. Moen, I., Bjerketvedt, D., Engebretsen, T., Jenssen, A., Hjertager, B.H. and Bakke, J.R., Transition to Detonation in a Flame Jet, *Comb. and Flame*, **75**, 1989, pp. 297-308.
11. Toedorczyk, A., Lee, J.H.S. and Knystautas, R., Propagation Mechanism of Quasi-Detonations, 22nd Symp. (Int.) on Combustion, Seattle, WA, The Combustion Inst., 1988, pp. 1723-1731.
12. Knystautas, R., Lee, J.H.S., Peraldi, O. and Chan, C.K., *Prog Astronaut. Aeronaut.*, **106**, 1986, pp. 37-52.
13. Zeldovich, Y.B., Librovich, V.B., Makhviladze, G.M., Sivashinskii, G.I., On the Onset of Detonation in a Nonuniformly Heated Gas, *J. Appl. Mech. Tech. Phys*., **11**, 1970, pp. 264–270.
14. Lee, J.H.S., Knystautas, R. and Yoshikawa, N. *Acta Astronaut*, **5**, 1978, pp. 971-982.
15. Ciccarelli, G. and Dorofeev, S., Flame Acceleration and Transition to Detonation in Ducts, *Progress in Energy and Combustion Science*, **34**, 2008, pp. 499-550.
16. Brennan, S., Makarov, D., and Molkov, V. LES of High Pressure Hydrogen Jet Fire. *Journal of Loss Prevention in the Process Industries*, **22**, No. 3, 2009, pp. 353-359.
17. Middha, P. Development, Use, and Validation of the CFD Tool FLACS for Hydrogen Safety Studies, PhD thesis, 2010, University of Bergen, Norway.
18. Gamezo, V.N., Ogawa, T. and Oran, E.S., Numerical Simulations of Flame Propagation and DDT in Obstructed Channels Filled with Hydrogen–Air Mixture, Proceedings of the Combustion Institute, **31**, No. 2, 2007, pp. 2463-2471.
19. Vaagaether, K., Knudsen, V. and Bjerketvedt, D., Simulation of Flame Acceleration and DDT in H_2-Air Mixture with a Flux Limiter Centred Method, Proceedings of the 1st International Conference on Hydrogen Safety, ICHS, 2005, Pisa, Italy.
20. Knudsen, V., Vaagsaether, K. and Bjerketvedt, D., An Experimental Study of Hydrogen-Air Gas Explosion in a Single Obstructed Pipe, Proceedings of the 1st Baltic Combustion Meeting, 2005.
21. Toro, E.F., Riemann Solvers and Numerical Methods for Fluid Dynamics: A Practical Introduction, 1999, Springer-Verlag, Berlin, Heidelberg.
22. Flohr, P. and Pitsch, H., Centre for Turbulent Research, Proceedings of the Summer Program, 2000.
23. Iijima, T. and Takeno, T., Effects of Temperature and Pressure on Burning Velocity, Proceedings of the Faculty of Engineering, Tokai Univ., **10**, 1984, pp. 53-67.
24. Korobeinikov, M.S., Levin, V.A., Markov, V.V. and Chernyi, G.G, Propagation of Blast in a Combustible Gas, *Astronautica Acta*, **17**, 1972, pp. 529-537.
25. Sichel, M., Tonello, N.A., Oran, E.S. and Jones, D.A., A Two–Step Kinetics Model for Numerical Simulation of Explosions and Detonations in H_2-O_2 Mixtures, *Proc. R. Soc. Lond. A*, **458**, 2002, pp. 49-82.
26. Del Alamo, G., Williams, F.A. and Sanchez, A.L., Hydrogen–Oxygen Induction Times Above Crossover Temperatures, *Combustion Science and Technology*, **176**, 2004, pp. 1599–1626.
27. Gaathaug, A.V., Bjerketvedt, D. and Vaagsaether, K., Experiments with Flame Propagation in a Channel with a Single Obstacle and Premixed Stoichiometric H_2-Air, *Combustion Science and Technology*, **182**, No. 11, 2010, pp. 1693-1706.
28. Dabora, E.K., Nicholls, J.A., and Morrison, R.B., The Influence of a Compressible Boundary Layer on the Propagation of Gaseous Detonations, 10th Symp. (Int.) on Combustion, The Combustion Inst., 1965, pp. 817-830.
29. Vaagsaether, K., Modelling of Gas Explosions, PhD thesis, 2010, Telemark University College – NTNU, 2010:221.